

Gas sensing properties and p-type response of ALD TiO₂ coated carbon nanotubes

Journal:	<i>Nanotechnology</i>
Manuscript ID:	NANO-104240.R2
Manuscript Type:	Special Issue Article
Date Submitted by the Author:	n/a
Complete List of Authors:	marichy, catherine; LMI - UMR5615 CNRS/Université de Lyon, Donato, Nicola; University of Messina, Electronic Engineering, Chemistry and Industrial Engineering Latino, Mariangela; University of Messina, Electronic Engineering, Chemistry and Industrial Engineering Willinger, Marc George; Fritz Haber Institute of the Max Planck Society, Department of Inorganic Chemistry Tessonnier, Jean-Philippe; Biorenewables Research Laboratory - Iowa State University, Chemical and Biological Engineering Neri, Giovanni; University of Messina, Electronic Engineering, Chemistry and Industrial Engineering Pinna, Nicola; Humboldt-Universität zu Berlin, Chemistry
Article Keywords:	atomic layer deposition, carbon nanotube, titanium dioxide, gas sensing, heterostructures
Abstract:	Amorphous titanium dioxide-coated carbon nanotubes were prepared by atomic layer deposition and investigated as sensing layers for resistive NO ₂ and O ₂ gas sensors. By varying ALD process conditions and CNT structure, heterostructures with different metal oxide grain size, morphology and coating thickness were synthesized. Higher responses were observed with homogeneous and continuous 5.5 nm thick films onto CNTs at an operating temperature of 150 °C, while CNTs decorated with either discontinuous film or TiO ₂ nanoparticles showed a weak response close to the one of device made of bare CNTs. An unexpected p-type behavior in presence of the target gas was also noticed, independently of the metal oxide morphology and thickness. Based on previous works, hypotheses were made in order to explain the p-type behavior of TiO ₂ /CNT sensors.

Gas sensing properties and p-type response of ALD TiO₂ coated carbon nanotubes

Catherine Marichy^{1*}, Nicola Donato², Mariangela Latino², Marc Georg Willinger³, Jean-Philippe Tessonnier⁴, Giovanni Neri², Nicola Pinna⁵

1 - Department of Chemistry, CICECO, University of Aveiro, 3810-193 Aveiro, Portugal.

Present address: LMI, CNRS UMR 5615, Université Lyon 1, 22 av. Gaston Berger - Bât. Berthollet, 69622 Cedex Villeurbanne, France.

2 - Department of Electronic Engineering, Chemistry and Industrial Engineering, University of Messina, Contrada di Dio, Vill. S. Agata, 98166, Messina, Italy.

3 - Department of Inorganic Chemistry, Fritz Haber Institute of the Max Planck Society, Faradayweg 4-6, 14195 Berlin, Germany.

4 - Biorenewables Research Laboratory, Department of Chemical and Biological Engineering, Iowa State University, Ames, Iowa 50011-3270, United States.

5 - Humboldt-Universität zu Berlin, Institut für Chemie, Brook-Taylor-Strasse 2, 12489 Berlin, Germany.

Email: catherine.marichy@univ-lyon1.fr

Abstract

Amorphous titanium dioxide-coated carbon nanotubes were prepared by atomic layer deposition and investigated as sensing layers for resistive NO₂ and O₂ gas sensors. By varying ALD process conditions and CNT structure, heterostructures with different metal oxide grain size, morphology and coating thickness were synthesized. Higher responses were observed with homogeneous and continuous 5.5 nm thick films onto CNTs at an operating temperature of 150 °C, while CNTs decorated with either discontinuous film or TiO₂ nanoparticles showed a weak response close to the one of device made of bare CNTs. An unexpected p-type behavior in presence of the target gas was also noticed, independently of the metal oxide morphology and thickness. Based on previous works, hypotheses were made in order to explain the p-type behavior of TiO₂/CNT sensors.

Keywords

Atomic layer deposition, carbon nanotube, titanium dioxide, gas sensing, heterostructures

Introduction

Based on the modification of their physical properties (e.g. electrical, optical) in presence of a target gas, chemical sensors find important application in everyday life. Indeed, they are widely applied to household security, industrial emission control, biomedical and agricultural domains, and to control

1
2
3 emission of engine combustion vehicles [1, 2]. In general, metal oxide semiconductors are used as
4 active layers in resistive sensors, SnO₂, ZnO and TiO₂ being widely used [3-5]. These sensors are very
5 attractive due to their high sensitivity, stability, low cost and fast response. Due to the strong
6 correlation between grain size and sensor response [6, 7], nanostructured and/or heterostructured
7 materials permit an enhancement of the gas sensing response. However, sensors based on metal oxide
8 semiconductor as sensing layer often operate at high temperature, which is a strong limitation for some
9 applications. Efforts have been devoted on combining metal oxides with a suitable conductive support
10 to develop near room temperature (RT) gas sensors with a reduced power consumption. Carbon
11 nanotubes (CNTs) appear as an ideal support for such applications due to their intrinsic electrical
12 properties, which can be influenced by the surrounding atmosphere. CNTs have been already
13 employed as support for various metal oxide sensing layer [8-14] and a recent paper described a
14 general sensing mechanism for SnO₂-carbon heterostructures [15].

15
16 Titanium dioxide is a wide-band gap semiconductor well-known as stable and highly reactive
17 photocatalyst. It is also used as gas sensor and especially one dimensional TiO₂ materials have been
18 intensively studied [16, 17]. Even though crystalline titanium oxide phases are mostly studied, few
19 papers demonstrated good sensing properties of amorphous TiO₂ nanotubes towards oxygen at
20 low/moderate temperature [18]. TiO₂/CNT hybrid composites have been already investigated as gas
21 sensors [19-26]. Early attempts focused on dispersion of CNTs into titania films [19, 21, 22].
22 Deposition of TiO₂ nanoparticles/film onto CNT walls was also studied [24-26]. However, good
23 conformality and homogeneity as well as a precise control of the thickness/particle size remain still
24 challenging. This requires a synthesis approach that is capable of controlling the decoration or
25 deposition on the support with an atomic scale precision, whilst preserving the support characteristic
26 properties. Atomic Layer Deposition (ALD) appears as one of the most promising techniques due to
27 its simplicity, reproducibility and high conformality of the obtained films. It has already been widely
28 used for nanostructured materials [27-31] and coating/decoration of carbon nanotubes [32]. TiO₂ ALD
29 has been successfully applied to the coating of CNTs [33-41], and the obtained structured materials
30 were employed for various applications such as solar cells [37, 39], photocatalysis [40], photodetector
31 [38] and capacitor [41]. The ALD technique was also already applied for tin dioxide/CNTs [9, 42, 43]
32 and vanadium oxide/CNTs [10] based gas sensors.

33
34 In this paper, sensing properties of controlled TiO₂/CNT nanostructures are reported. ALD was used to
35 prepare the sensing material with a precise control of the morphology and size of the metal oxide
36 deposited onto outer and inner parts of the CNTs. An unexpected p-type response towards nitrogen
37 dioxide and oxygen was observed. Indeed, TiO₂ generally behaves as n-type semiconducting material
38 and, in this form, was well studied and extensively used as sensing element in chemoresistor devices
39 for gas sensing applications. On the other hand, very few recent reports can be found on pure and
40 doped-TiO₂ p-type materials [23, 44, 45]. Because a switch between the two material typology
41 involves a change of dominating surface species and surface chemical reactions determining the

1
2
3 sensing mechanism, this study could give new insight about the general understanding of sensing
4 mechanism on p-type hybrid semiconducting materials. Based on the previous sensing mechanism
5 established for SnO₂-carbon structures [15], an attempt is made to explain this behavior.
6
7
8

9 **Methods**

10 Different grades of cup-stacked CNTs (Pyrograf III: PR-24-PS, PR-24-LHT and PR-24-HHT), were
11 coated with TiO₂ by ALD. Depending of their type, CNTs were pre-treated in inert atmosphere,
12 respectively, at either 700, 1500 or 3000 °C [46] leading to various degrees of graphitization and
13 subsequently to different degrees of functionalization of the tube walls. Details on CNTs [47] and
14 CNT coating are described elsewhere [48]. Briefly, prior ALD, nitric acid (70 %) treatment for 10h at
15 100 °C was realized on the different types of CNTs. After functionalization, for the sake of clarity
16 CNTs PR-24-PS, PS-24-LHT and PR-24-HHT are labeled CNT700, CNT1500 and CNT3000,
17 respectively. Each type of CNTs was deposited by drop-casting on a silicon wafer from dispersions in
18 ethanol. After sample drying at 200 °C under vacuum for one hour, titanium dioxide was deposited in
19 a home-made ALD reactor working in exposure mode at 200 °C from titanium isopropoxide and
20 acetic acid [34]. The three different grades of CNTs and a reference Si wafer were coated
21 simultaneously. The number of cycles was chosen between 50 and 500 in order to have a metal oxide
22 thickness ranging from 1.5 to 15 nm on CNTs, considering a nominal growth per cycle of 0.6 Å on Si
23 substrate.
24

25 ALD deposition was verified with thickness measurement of the as-deposited metal oxide films on
26 wafer substrates. X-ray reflectivity was performed using a Phillips X'Pert MRD X-ray diffractometer
27 with a copper radiation and a graphite monochromator for the selection of pure K α radiation. Obtained
28 TiO₂-CNT heterostructures were characterized by high-resolution transmission electron microscopy
29 (HRTEM) and scanning transmission electron microscopy (STEM) using a JEOL EM-2010, a JEOL
30 JEM-2200FS, a Hitachi H9000 and a Philips CM200 FEG microscope. Scanning electron microscopy
31 (SEM) images were recorded using a FEG-SEM Hitachi SU-70 microscope operating at 4 kV with a
32 working distance of 2-3 mm. SEM and TEM investigations were carried out on copper TEM grids
33 with a holy carbon support film. The samples were deposited by dipping the TEM grids into dry
34 powder.
35

36 Home-made sensing device used for gas testing consists of an alumina substrate with Pt interdigitated
37 electrodes on one side, and a Pt heater on the other side. The spacing between Pt electrodes measures
38 200 microns. The active sensing layer was deposited by screen printing of an aqueous solution with
39 coated carbon nanotubes. Gas sensing tests were carried out inside a stainless-steel chamber under
40 controlled atmosphere. Mass flow controllers were used to adjust desired concentrations of target
41 gases in dry air. Electrical and sensing measurements were carried out in the temperature range from
42 RT to 250 °C, with steps of 50 °C under a dry nitrogen/air total flow of 50 sccm. The sensor response
43 was measured as change in resistance in four point mode using an Agilent 34970A multimeter. An
44
45
46
47
48
49
50
51
52
53
54
55
56
57
58
59
60

1
2
3 Agilent E3632A dual-channel power supply was used for the heater of the sensor. The sensors were
4 tested for monitoring NO₂ and O₂. The response of the gas sensor is defined as $S = R_0/R_{gas}$ where R_0
5 is the baseline resistance and R_{gas} is the electric resistance of the sensor at different target gas
6 concentration. To perform the resistance measurement, the instrument is biased at a constant current
7 value (10 μA, settled taking into account the resistance of the sensor, approximately 20 - 60 kΩ) and
8 reading the voltage across the sensors.
9
10
11
12

13 14 15 **Results and Discussion**

16 The fabrication and structural characterizations of these hetero-structures were already extensively
17 reported elsewhere [48]. Different TiO₂ morphologies were obtained depending on the structural
18 characteristics of the support. It was established that the density and nature of the surface oxygen-
19 containing functional groups produced by nitric acid functionalization vary with the graphitic
20 character of the nanotubes. A higher concentration of phenolic and carboxylic acids groups were
21 observed when decreasing the graphitic character [49]. A detailed morphological and structural
22 characterization of the various carbon nanotubes treated at various temperatures has been reported
23 elsewhere [47, 49].
24
25
26
27
28

29 Atomic layer deposition is based on self-limiting surface reactions and film growth requires the
30 presence of anchoring sites to initiate [50, 51]. Controlled change of surface functionality of the CNTs
31 allows tailoring metal oxide morphologies. A homogeneous and conformal amorphous TiO₂ film was
32 deposited onto CNT700 (**Figure 1a, d**), while amorphous titanium oxide grown on CNT1500 (Figure
33 1b, e) and CNT3000 (Figure 1c, f) have a more granular aspect and a pronounced particulate structure
34 on the inner and outer walls of the carbon material [48]. In case of CNT1500, even though a transition
35 from an island to a 2D growth is observed with an increase of the number of cycles, large uncoated
36 areas (Figure 1e) remain. They are attributed to carbon inertness and not only to eventual contact point
37 during the coating. As previously described, the structure of CNT3000 tubes is made of steps, walls
38 and flat terraces that are highly graphitized [49]. Thus the titania growth occurs preferentially at the
39 edges of connected cones while the highly graphitized regions remain almost uncoated, leading to the
40 formation of rings of TiO₂ film wrapped around the CNTs as nicely shown in the low resolution TEM
41 image in Figure 1f [48]. Metal oxide layer thickness was modulated by changing the number of ALD
42 cycles. The effective deposited thickness was determined by TEM imaging.
43
44
45
46
47
48
49
50
51
52
53
54
55
56
57
58
59
60

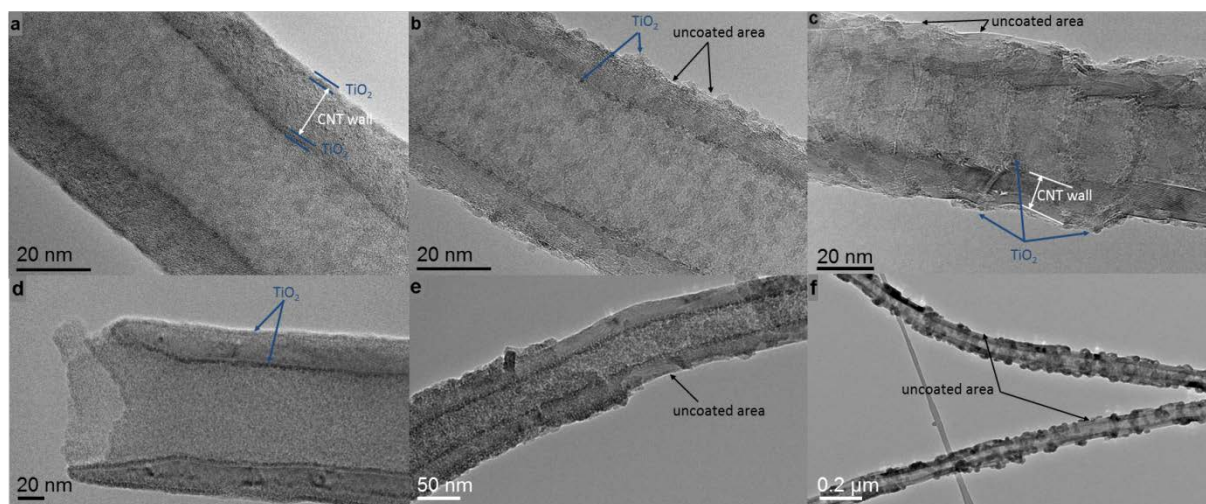


Figure 1. TEM images of CNTs coated with 50 (a, b, c) and 400 (d, e, f) ALD cycles of TiO₂. (a, d) CNT700, (b, e) CNT1500, (c, f) CNT3000. Film thickness and particle diameter are approximately 2 and 9 nm after 50 and 400 cycles, respectively

Electrical properties and sensing behavior on devices made of pure CNTs were already described elsewhere [15]. Electrical measurements performed on TiO₂ sensing materials served as reference and baseline for the gas sensing tests. Although the baseline resistance of TiO₂/CNT sensors is higher than that of bare CNTs (50-150 Ω), it is much lower than that of pure TiO₂. As shown in **Figure 2a**, the resistance of a thick film made of TiO₂ nanoparticles is in the MΩ range, reflecting its insulating character, while the resistance of TiO₂/CNT700 is measurable (10³-10⁴ Ω) even at room temperature and decreases with rising temperature, indicating a semiconductor behavior. Specifically, as CNTs are coaxially coated, the shell of TiO₂ should create high contact resistance at crossing points. However, due to the low TiO₂ thickness, tunneling effect can overcome this limitation reducing the height of the potential barrier for the conduction at crossing points, whereas CNT cores provide a privileged conduction path. Similar behavior was already observed for sensing layer made of SnO₂-coated carbon nanotubes [9, 15]. The resistance of the hetero-structures is dependent of the oxide thickness, with a maximum for 5.5 nm TiO₂ (Figure 2b). In order to explain the observed behavior, one would consider that, other than the tunneling mechanism, the resistance is dominated by the Schottky barrier at the metal oxide film surface. Thus, the resistance of the device should be higher when the oxide layer is fully depleted, i.e. when the thickness of the TiO₂ film is comparable to the Debye length (L_d , about 11 nm for TiO₂ at 250 °C) [52], as oxygen gas adsorption at the surface induces a complete depletion of carriers in the nanostructures. On the other hand, at the lowest TiO₂ thickness, tunneling effect can overcome this limitation reducing the height of potential barrier for the conduction at crossing points. Increasing the TiO₂ thickness up to 4-7 nm causes an increase of resistance because the tunneling mechanism just vanishes within few nanometers while the oxide layers are still fully depleted. Coating

thickness exceeding 8 nm causes the resistance to decrease, indicating that the conduction mechanism is not dominated by the Schottky barrier anymore.

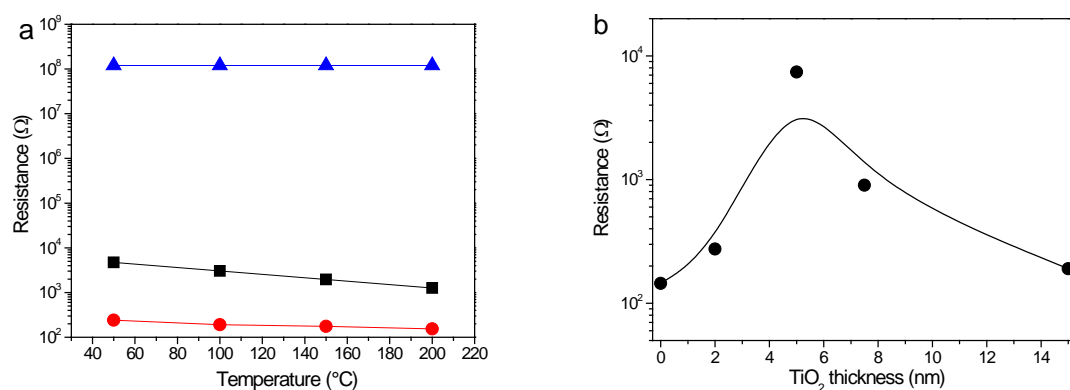


Figure 2. a) Resistance as a function of the temperature of the sensor devices made of pure CNT700 (circles), TiO₂/CNT700 (squares) and pure TiO₂ (triangles). b) Resistance of TiO₂/CNT700 sensor device as a function of the metal oxide sensing layer thickness at the temperature of 150 °C.

Figure 3a shows the response of TiO₂/CNT700 and TiO₂/CNT3000 devices as a function of the operating temperature. Although responses of both sensors are relatively weak in the whole range of temperature studied, the response of TiO₂/CNT3000 sensor remains nearly constant similarly to the sensing behavior of uncoated CNT film (see **Figure S1a** in Supporting Information), while the one of TiO₂/CNT700 sensor is strongly influenced by the operating temperature. A measurable response is already observed at near room temperature (40 °C), showing a maximum around 100-150 °C. The dynamic responses of TiO₂/CNT700, TiO₂/CNT1500 and TiO₂/CNT3000 hetero-structure sensors to 8 ppm NO₂ are presented in Figure 3b-d. The magnitude of the resistance modification upon NO₂ exposure clearly depends on the CNT support (the response of devices made of uncoated CNT700 and CNT1500 are shown in Figure S1 in SI), the response of TiO₂/CNT700 (Figure 3b) being approximately 3-8 times higher than those of the other sensors. The sensor resistance decreases in presence of the target gas for all sensors reflecting a p-type semiconductor character. Longer response and recovery times can also be noted when CNT3000 is used as support.

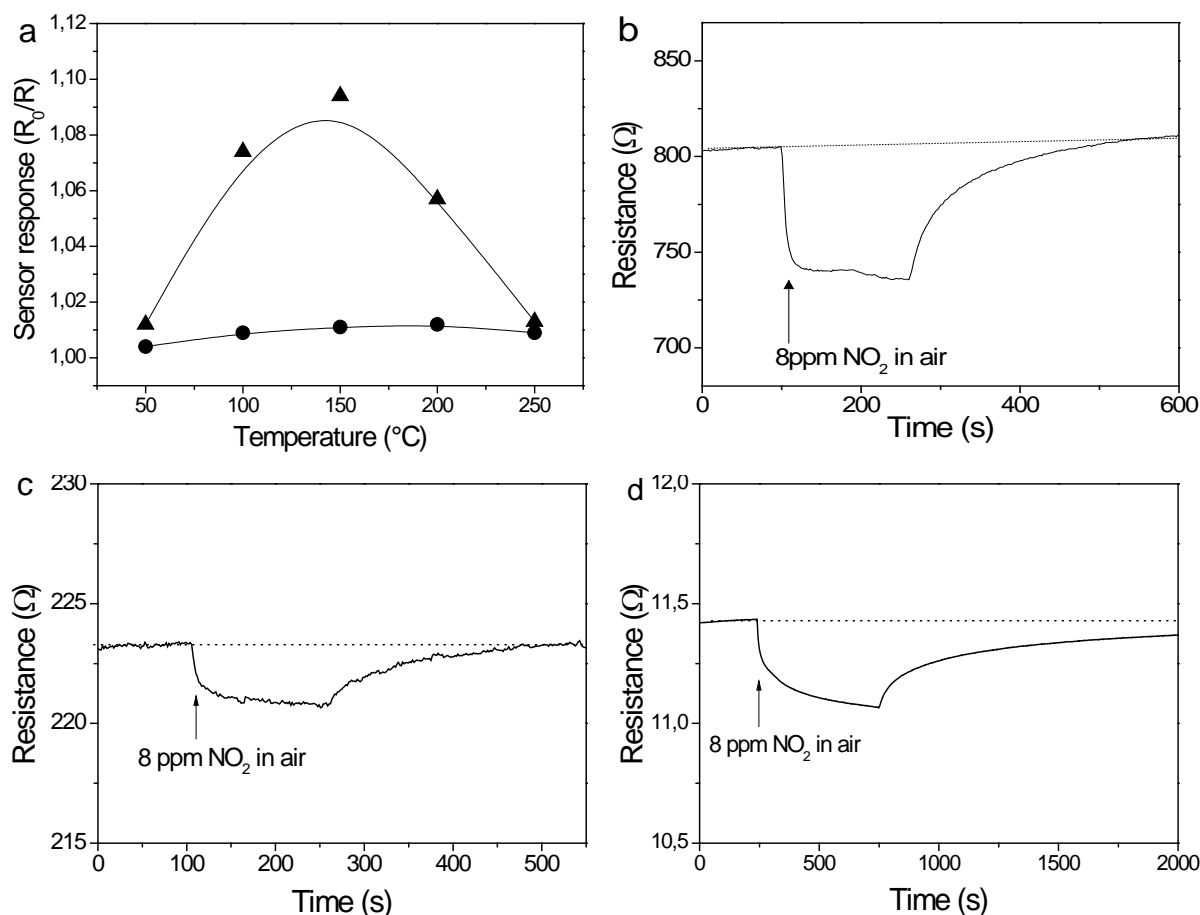


Figure 3. a) Sensor responses, toward 8 ppm of NO₂, as a function of the operating temperature, of 8 nm TiO₂/CNT700 (triangles) and 9 nm TiO₂/CNT1500 (dots) sensors. Transient responses to 8 ppm of NO₂ at 150 °C of devices made of b) 8 nm TiO₂/CNT700, c) 9 nm TiO₂/CNT1500 and d) 10 nm sized TiO₂ particles-decorated CNT3000.

The influence of TiO₂ thickness on the sensing properties was investigated by simple control of the number of ALD cycles performed. **Figure 4a** shows the response towards NO₂ of sensors consisting of CNT700 coated with various TiO₂ cycles. The response is influenced by the metal oxide thickness and presents a maximum at ~5.5 nm titania film. The same trend was obtained with TiO₂/CNT1500 and TiO₂/CNT3000. The influence of oxide thickness on the sensing response can be explained by the space charge layer model [53]. When the MO_x layer is in the range of the space charge region, i.e. the thickness is reduced down to the Debye length, the space charge layer is fully depleted and thus higher sensitivity is obtained [6]. It can be noted that the sensor response increases as the TiO₂ layer baseline resistance increases too (Figure 4b), indicating a correlation between these two parameters.

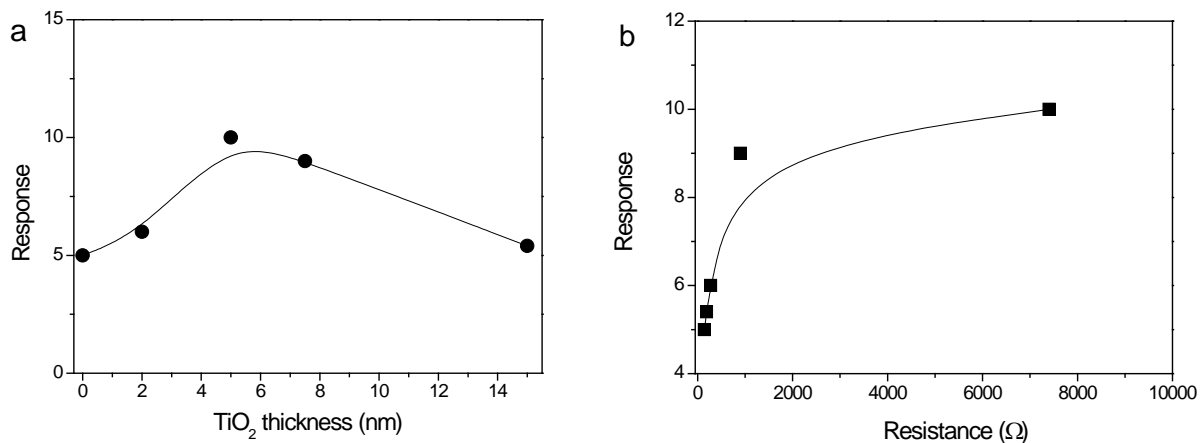


Figure 4. a) Sensing response of TiO₂/CNT700 sensor devices towards 8 ppm of NO₂ at 150 °C as a function of the thickness of the TiO₂ sensing layer and b) Sensing response of TiO₂:CNT700 as a function of the device baseline resistance.

The values of τ_{res} and τ_{rec} , *i.e.* the response and recovery times, respectively, of TiO₂/CNT700 sensors as a function of the operating temperature are presented in **Figure 5**. One can clearly observe that both dynamic parameters of the sensor strongly decrease with the temperature and that the response is much faster than the recovery. At near room temperature, the sensor responds in less than 4 minutes.

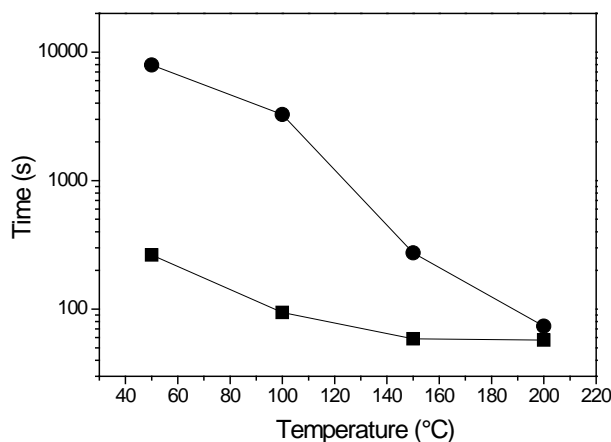
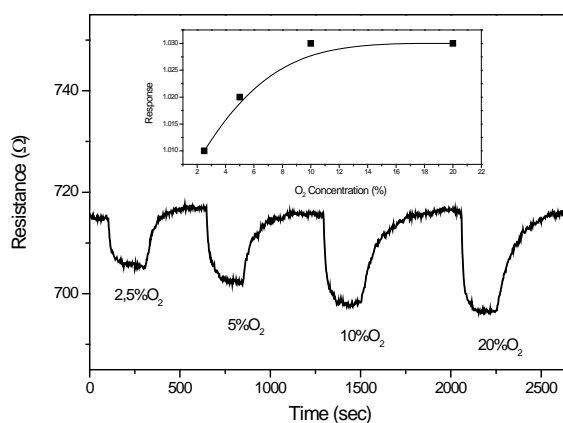


Figure 5. Response (squares) and recovery (dots) times of TiO₂/CNT700 sensors to 5 ppm of NO₂ as a function of the operating temperature.

The data reported for NO₂ sensing suggest a p-type semiconductor character. However, as NO₂ can behave as an oxidizing or reducing gas depending on temperature and concentration, additional experiments were performed on TiO₂/CNT700, using oxygen as target gas, in order to avoid a misinterpretation of the semiconductor type. The literature data agree with an increase of the electrical resistance under exposure to O₂, in accordance with a n-type character of titania in the anatase phase. On the other hand, the rutile phase exhibits p-type character [54].

1
2
3 The data presented here showed that a decrease of the sensor resistance occurs in the presence of
4 oxygen, as for NO₂ sensing. Transient response of the 8 nm TiO₂/CNT700 sensor towards different
5 concentrations of O₂ in nitrogen at 150 °C (**Figure 6**) confirms the p-type character of the
6 nanostructured sensors. This indicates that when NO₂/O₂ adsorbs on the titania active layer, the
7 electrons are transferred to the NO₂/O₂ molecule, which in turn causes an effective electronic charge
8 transfer from the carbon nanotube to the titania coating, decreasing the overall resistance of the
9 heterostructured sensor device. The calibration curve shows a linear response up to 10 v/v (%) of O₂ in
10 nitrogen, afterwards a saturation level is reached.
11
12
13
14
15
16
17



18
19
20
21
22
23
24
25
26
27
28
29
30
31
32
33 **Figure 6.** Transient response of 8 nm TiO₂/CNT700 towards different concentrations of O₂ in nitrogen
34 at 150 °C. Inset shows the calibration curve.
35

36
37 Even though some works [23, 44] reported the p-type behavior of titanium dioxide, it is usually
38 considered as a n-type semiconductor. Previously, we investigated the oxygen sensing mechanism of
39 thick films of TiO₂ nanoparticles; data showed an increase of the resistance with oxygen
40 concentration, demonstrating a n-type sensing mechanism [55]. Different sensing mechanism of
41 carbon nanotube-TiO₂ hybrid composites are reported in literature, depending on the target gas,
42 operating temperature, synthesis method, thermal treatment, morphological and structural
43 characteristics. Bittencourt et al. reported that multiwalled CNTs/metal oxide films behave either as p-
44 type or n-type semiconductor depending on the loading of CNTs dispersed into the metal oxide matrix
45 [56]. Carbon nanotube-TiO₂ hybrid films showed an increasing resistance in presence of O₂, revealing
46 a n-type response of the hetero-structure. An enhanced sensitivity, attributed to the formation of a
47 heterojunction, was also noted, compared to optimized Nb-doped TiO₂ sensing device [19]. The same
48 behavior has been observed previously by us with electrospun CNTs/PVAc/TiO₂ composites [57]. On
49 the other hand, a n- to p-behavior transition has been reported for electrospun TiO₂ nanofibers at high
50 NO₂ concentration [58]. An influence of the operating temperature and the target gas concentration on
51 the response and on the n- to p-character transition was observed and attributed to a change of carrier
52 density in the sensing material made of ZnO nanotubes [59]. Sánchez *et al.* [23] found an anomalous
53
54
55
56
57
58
59
60

1
2
3 p-type behavior in the interaction of NH_3 with TiO_2 films annealed at $400\text{ }^\circ\text{C}$, whereas identical films
4 annealed at $600\text{ }^\circ\text{C}$ showed the expected n-type response. The experimental data, together with
5 theoretical calculations, suggested that the different responses were associated to different geometrical
6 and chemical environments around the adsorption sites on the surface of the films annealed at different
7 temperature. More specifically, when the surface was rich in Ti sites of low coordination and OH
8 groups (expected in films annealed at lower temperatures), the dissociation of the NH_3 molecules was
9 facilitated, which could promote a charge transfer from the metal oxide to the ammonia molecule. The
10 same group reported a difference of character of MWCNT- TiO_2 as a function of the preparation
11 method. Screen-printed sensor presented a p-type response toward NH_3 while the dip-coated one
12 showed a n-type behavior. This phenomenon was attributed to a larger concentration of Ti^{3+} in dip
13 coating film and/or difference in coordination environment of Ti [22]. A similar phenomenon could be
14 therefore responsible for the type of response observed with the TiO_2/CNT materials produced by
15 ALD at $200\text{ }^\circ\text{C}$.
16

17 All the TiO_2/CNT sensors studied here exhibit instead a clear p-type response in the whole range of
18 investigated concentration of the target gases, regardless of the film morphology or thickness, which
19 indicates that the morphology of the film is not responsible for the p-type response observed. Then, it
20 is plausible to attribute the observed n- to p-type transition to the presence of CNTs.
21

22 A general sensing mechanism of tin dioxide-carbon heterostructure devices has been recently
23 suggested [15]. The role of the different junctions involved in the response were established: the
24 enhanced response was attributed to the formation of a p-n heterojunction between the metal oxide
25 film and carbon support, modulated through the modification of the energy barrier occurring between
26 two SnO_2 films in contact and where the CNT core provides mainly the electronic conduction path.
27 Although all the TiO_2/CNT sensors exhibit a relatively weak response towards NO_2 , those of
28 $\text{TiO}_2/\text{CNT1500}$ and $\text{TiO}_2/\text{CNT3000}$ are weaker than that of $\text{TiO}_2/\text{CNT700}$. Like for the influence of
29 the CNT type on the sensing behavior of SnO_2/CNTs , those results can be explained by the presence
30 of large CNT uncoated areas on the former sensors, leading to dominating carbon/carbon junctions,
31 responsible for a weaker response, and response and recovery times. Furthermore, the unusual p-type
32 response of TiO_2/CNT sensors give more insight on the importance of the metal oxide/metal oxide
33 junction. Indeed, the observed sensing response could arise from the nature of the homojunction
34 between the metal oxide of two coated carbon supports determining the type of response (i.e. p- or n-
35 type) of the device. Based on it, if the contact between the coatings leads to n-junction, a response of
36 the same type will be observed while the opposite behavior will be observed if a p-junction is formed.
37 Hall measurement, yielding the sheet carrier density, n_s , and the bulk density and mobility of n or p
38 carriers, could give helpful indications to clarify the sensing mechanism.
39
40
41
42
43
44
45
46
47
48
49
50
51
52
53
54
55
56
57
58
59
60

Conclusion

1
2
3 Ultra-thin titanium dioxide coatings were formed onto carbon nanotubes in a controlled manner by
4 nonaqueous sol-gel ALD approach. Continuous and conformal layers, granular coatings or only
5 dispersed nanoparticles were formed as a function of the CNT grade used. The heterostructures,
6 deposited onto alumina substrate and provided with interdigitated electrodes, were investigated as
7 resistive gas sensors. Unexpectedly the sensors devices show p-type response to nitrogen dioxide and
8 a low optimal operating temperature of 150 °C. A significant change of resistivity in presence of target
9 gas was only obtained for continuous titanium dioxide film onto CNT700. Similar mechanism as for
10 SnO₂/CNT and V₂O₅/CNT seems to be involved in the present sensing process. The synergic effect,
11 due to the interface between the film and support, highly depends of the TiO₂ film thickness and
12 morphology. Highest sensitivity and sensor responses are observed for continuous film with
13 thicknesses in the range of the TiO₂ Debye length. Hypotheses have been formulated in order to
14 explain the appearance of the p-type conductivity and the sensing behavior toward NO₂ and O₂. These
15 TiO₂/CNT-based devices would certainly be of interest for sensing other target gas toward which TiO₂
16 already shown more sensitivity such acetone and alcohols. The formed heterojunction might allow a
17 reduced operating temperature.
18
19
20
21
22
23
24
25
26
27
28

29 **Acknowledgements**

30 This work was partially supported by the FCT projects (PTDC/CTM/098361/2008),
31 (PTDC/CTM/100468/2008), and (REDE/1509/RME/2005) and the FCT grant
32 (SFRH/BD/71453/2010).
33
34
35
36

37 **References**

- 38
39 [1] G. Neri, *Sci. Adv. Mater.*, 2 (2010) 3-15.
40 [2] A. Tricoli, M. Righettoni, A. Teleki, *Angew. Chem. Int. Ed.*, 49 (2010) 7632-7659.
41 [3] G. Korotcenkov, *Mater. Sci. Eng. R: Rep.*, 61 (2008) 1-39.
42 [4] W. Gopel, K.D. Schierbaum, *Sens. Actuators, B*, 26 (1995) 1-12.
43 [5] M. Batzill, *Sensors*, 6 (2006) 1345-1366.
44 [6] C. Xu, J. Tamaki, N. Miura, N. Yamazoe, *Sens. Actuators, B*, 3 (1991) 147-155.
45 [7] G.F. Fine, L.M. Cavanagh, A. Afonja, R. Binions, *Sensors*, 10 (2010) 5469-5502.
46 [8] B.-Y. Wei, M.-C. Hsu, P.-G. Su, H.-M. Lin, R.-J. Wu, H.-J. Lai, *Sens. Actuators, B*, 101 (2004)
47 81-89.
48 [9] C. Marichy, N. Donato, M.-G. Willinger, M. Latino, D. Karpinsky, S.-H. Yu, G. Neri, N. Pinna,
49 *Adv. Funct. Mater.*, 21 (2011) 658-666.
50 [10] M.G. Willinger, G. Neri, E. Rauwel, A. Bonavita, G. Micali, N. Pinna, *Nano Lett.*, 8 (2008) 4201-
51 4204.
52 [11] H. Zhao, B. Rizal, G. McMahon, H. Wang, P. Dhakal, T. Kirkpatrick, Z. Ren, T.C. Chiles, M.J.
53 Naughton, D. Cai, *ACS Nano*, 6 (2012) 3171-3178.
54 [12] W. Li, H. Jung, N.D. Hoa, D. Kim, S.-K. Hong, H. Kim, *Sens. Actuators, B*, 150 (2010) 160-166.
55 [13] S. Santangelo, G. Messina, G. Faggio, M.G. Willinger, N. Pinna, A. Donato, A. Arena, N.
56 Donato, G. Neri, *Diamond Relat. Mater.*, 19 (2010) 590-594.
57 [14] N.D. Hoa, N. Van Quy, D. Kim, *Sens. Actuators, B*, 142 (2009) 253-259.
58 [15] C. Marichy, P.A. Russo, M. Latino, J.-P. Tessonier, M.-G. Willinger, N. Donato, G. Neri, N.
59 Pinna, *J. Phys. Chem. C*, 117 (2013) 19729-19739.
60

- 1
2
3 [16] M.M. Arafat, B. Dinan, S.A. Akbar, A.S. Haseeb, *Sensors* (Basel, Switzerland), 12 (2012) 7207-
4 7258.
5 [17] V. Galstyan, E. Comini, G. Faglia, G. Sberveglieri, *Sensors*, 13 (2013) 14813-14838.
6 [18] L. Hao Feng, L. Feng, L. Gang, C. Zhi-Gang, W. Da-Wei, F. Hai-Tao, L. Gao Qing, J. Zhou Hua,
7 C. Hui-Ming, *Nanotechnology*, 19 (2008) 405504.
8 [19] E. Llobet, E.H. Espinosa, E. Sotter, R. Ionescu, X. Vilanova, J. Torres, A. Felten, J.J. Pireaux, X.
9 Ke, G.V. Tendeloo, F. Renaux, Y. Paint, M. Hecq, C. Bittencourt, *Nanotechnology*, 19 (2008) 375501.
10 [20] E.H. Espinosa, R. Ionescu, B. Chambon, G. Bedis, E. Sotter, C. Bittencourt, A. Felten, J.J.
11 Pireaux, X. Correig, E. Llobet, *Sens. Actuators, B*, 127 (2007) 137-142.
12 [21] M. Sánchez, R. Guirado, M.E. Rincón, *J. Mater. Sci.:Mater. Electron.*, 18 (2007) 1131-1136.
13 [22] M. Sánchez, M.E. Rincón, *Sens. Actuators, B*, 140 (2009) 17-23.
14 [23] M. Sánchez, M.E. Rincón, R.A. Guirado-López, *J. Phys. Chem. C*, 113 (2009) 21635-21641.
15 [24] T. Ueda, K. Takahashi, F. Mitsugi, T. Ikegami, *Diamond Relat. Mater.*, 18 (2009) 493-496.
16 [25] S. Mun, Y. Chen, J. Kim, *Sens. Actuators, B*, 171-172 (2012) 1186-1191.
17 [26] H. Liu, H. Ma, W. Zhou, W. Liu, Z. Jie, X. Li, *Appl. Surf. Sci.*, 258 (2012) 1991-1994.
18 [27] S.M. George, *Chem. Rev.*, 110 (2010) 111-131.
19 [28] M. Knez, K. Nielsch, L. Niinistö, *Adv. Mater.*, 19 (2007) 3425-3438.
20 [29] M. Leskelä, M. Ritala, *Angew. Chem. Int. Ed.*, 42 (2003) 5548-5554.
21 [30] C. Marichy, M. Bechelany, N. Pinna, *Adv. Mater.*, 24 (2012) 1017-1032.
22 [31] N. Pinna, M. Knez, *Atomic Layer Deposition of Nanostructured Materials*, Wiley-VCH, 2011.
23 [32] C. Marichy, N. Pinna, *Coordination Chemistry Reviews*, 257 (2013) 3232-3253.
24 [33] E. Rauwel, G. Clavel, M.G. Willinger, P. Rauwel, N. Pinna, *Angew. Chem. Int. Ed.*, 47 (2008)
25 3592-3595.
26 [34] E. Rauwel, M.G. Willinger, F. Ducroquet, P. Rauwel, I. Matko, D. Kiselev, N. Pinna, *J. Phys.*
27 *Chem. C*, 112 (2008) 12754-12759.
28 [35] M.G. Willinger, G. Neri, A. Bonavita, G. Micali, E. Rauwel, T. Hertrich, N. Pinna, *Phys. Chem.*
29 *Chem. Phys.*, 11 (2009) 3615-3622.
30 [36] A. Gomathi, S.R.C. Vivekchand, A. Govindaraj, C.N.R. Rao, *Adv. Mater.*, 17 (2005) 2757-2761.
31 [37] S.H. Jin, G.H. Jun, S.H. Hong, S. Jeon, *Carbon*, 50 (2012) 4483-4488.
32 [38] C.-Y. Hsu, D.-H. Lien, S.-Y. Lu, C.-Y. Chen, C.-F. Kang, Y.-L. Chueh, W.-K. Hsu, J.-H. He,
33 *ACS Nano*, 6 (2012) 6687-6692.
34 [39] C.L. Pint, K. Takei, R. Kapadia, M. Zheng, A.C. Ford, J. Zhang, A. Jamshidi, R. Bardhan, J.J.
35 Urban, M. Wu, J.W. Ager, M.M. Oye, A. Javey, *Adv. Energy Mater.*, 1 (2011) 1040-1045.
36 [40] S. Deng, S.W. Verbruggen, Z. He, D.J. Cott, P.M. Vereecken, J.A. Martens, S. Bals, S. Lenaerts,
37 C. Detavernier, *RSC Adv.*, 4 (2014) 11648-11653.
38 [41] X. Sun, M. Xie, J.J. Travis, G. Wang, H. Sun, J. Lian, S.M. George, *J. Phys. Chem. C*, 117 (2013)
39 22497-22508.
40 [42] N. Donato, M. Latino, G. Neri, D. Spadaro, C. Marichy, M.-G. Willinger, N. Pinna, in: S.
41 Scalsese, A.L. Magna (Eds.) *2nd Carbomat Workshop*, Catania, 2011, pp. 37-40.
42 [43] N. Pinna, C. Marichy, M.G. Willinger, N. Donato, M. Latino, G. Neri, A. D'Amico, C.D. Di
43 Natale, L. Mosiello, G. Zappa, *Sensing Properties of SnO₂/CNFs Hetero-Junctions*
44 *Sensors and Microsystems*, in, Springer US, 2012, pp. 105-108.
45 [44] F. Hossein-Babaei, M. Keshmiri, M. Kakavand, T. Troczynski, *Sens. Actuators, B*, 110 (2005)
46 28-35.
47 [45] A. Wisitsoraat, A. Tuantranont, E. Comini, G. Sberveglieri, W. Wlodarski, *Thin Solid Films*, 517
48 (2009) 2775-2780.
49 [46] AppliedSciencesInc, in, 2011.
50 [47] J.-P. Tessonier, D. Rosenthal, T.W. Hansen, C. Hess, M.E. Schuster, R. Blume, F. Girgsdies, N.
51 Pfänder, O. Timpe, D.S. Su, R. Schlögl, *Carbon*, 47 (2009) 1779-1798.
52 [48] C. Marichy, J.-P. Tessonier, M.C. Ferro, K.-H. Lee, R. Schlögl, N. Pinna, M.-G. Willinger, *J.*
53 *Mater. Chem.*, 22 (2012) 7323-7330.
54 [49] J.-P. Tessonier, D. Rosenthal, F. Girgsdies, J. Amadou, D. Begin, C. Pham-Huu, D. Sheng Su,
55 R. Schlögl, *Chem. Commun.*, (2009) 7158-7160.
56
57
58
59
60

- 1
2
3 [50] Y.-S. Min, E.J. Bae, J.B. Park, U.J. Kim, W. Park, J. Song, C.S. Hwang, N. Park, *Appl. Phys.*
4 *Lett.*, 90 (2007) 263104-263103.
5 [51] X.R. Wang, S.M. Tabakman, H.J. Dai, *J. Am. Chem. Soc.*, 130 (2008) 8152-8153.
6 [52] V.V. Sysoev, B.K. Button, K. Wepsiec, S. Dmitriev, A. Kolmakov, *Nano Lett.*, 6 (2006) 1584-
7 1588.
8 [53] H. Ogawa, M. Nishikawa, A. Abe, *J. Appl. Phys.*, 53 (1982) 4448-4455.
9 [54] X. Li, R. Ramasamy, P.K. Dutta, *Sens. Actuators, B*, 143 (2009) 308-315.
10 [55] G. Neri, A. Bonavita, G. Micali, G. Rizzo, *ECS Trans.*, 3 (2006) 221-231.
11 [56] C. Bittencourt, A. Felten, E.H. Espinosa, R. Ionescu, E. Llobet, X. Correig, J.J. Pireaux, *Sens.*
12 *Actuators, B*, 115 (2006) 33-41.
13 [57] P. Frontera, S. Trocino, A. Donato, P.L. Antonucci, M. Lo Faro, G. Squadrito, G. Neri, *Electron.*
14 *Mater. Lett.*, 10 (2014) 305-313.
15 [58] I.-D. Kim, A. Rothschild, B.H. Lee, D.Y. Kim, S.M. Jo, H.L. Tuller, *Nano Lett.*, 6 (2006) 2009-
16 2013.
17 [59] J.X. Wang, X.W. Sun, Y. Yang, C.M.L. Wu, *Nanotechnology*, 20 (2009) 465501.
18
19
20
21
22
23
24
25
26
27
28
29
30
31
32
33
34
35
36
37
38
39
40
41
42
43
44
45
46
47
48
49
50
51
52
53
54
55
56
57
58
59
60

Supporting Information

Gas sensing properties and p-type response of ALD TiO₂ coated carbon nanotubes

Catherine Marichy^{1*}, Nicola Donato², Mariangela Latino², Marc Georg Willinger³, Jean-Philippe Tessonnier⁴, Giovanni Neri², Nicola Pinna⁵

1 - Department of Chemistry, CICECO, University of Aveiro, 3810-193 Aveiro, Portugal.

Present address: LMI, CNRS UMR 5615, Université Lyon 1, 22 av. Gaston Berger - Bât. Berthollet, 69622 Cedex Villeurbanne, France.

2 - Department of Electronic Engineering, Chemistry and Industrial Engineering, University of Messina, Contrada di Dio, Vill. S. Agata, 98166, Messina, Italy.

3 – Department of Inorganic Chemistry, Fritz Haber Institute of the Max Planck Society, Faradayweg 4-6, 14195 Berlin, Germany.

4 – Biorenewables Research Laboratory, Department of Chemical and Biological Engineering, Iowa State University, Ames, Iowa 50011-3270, United States.

5 - Humboldt-Universität zu Berlin, Institut für Chemie, Brook-Taylor-Strasse 2, 12489 Berlin, Germany.

Email: catherine.marichy@univ-lyon1.fr

Keywords

Atomic layer deposition, carbon nanotube, titanium dioxide, gas sensing, heterostructures

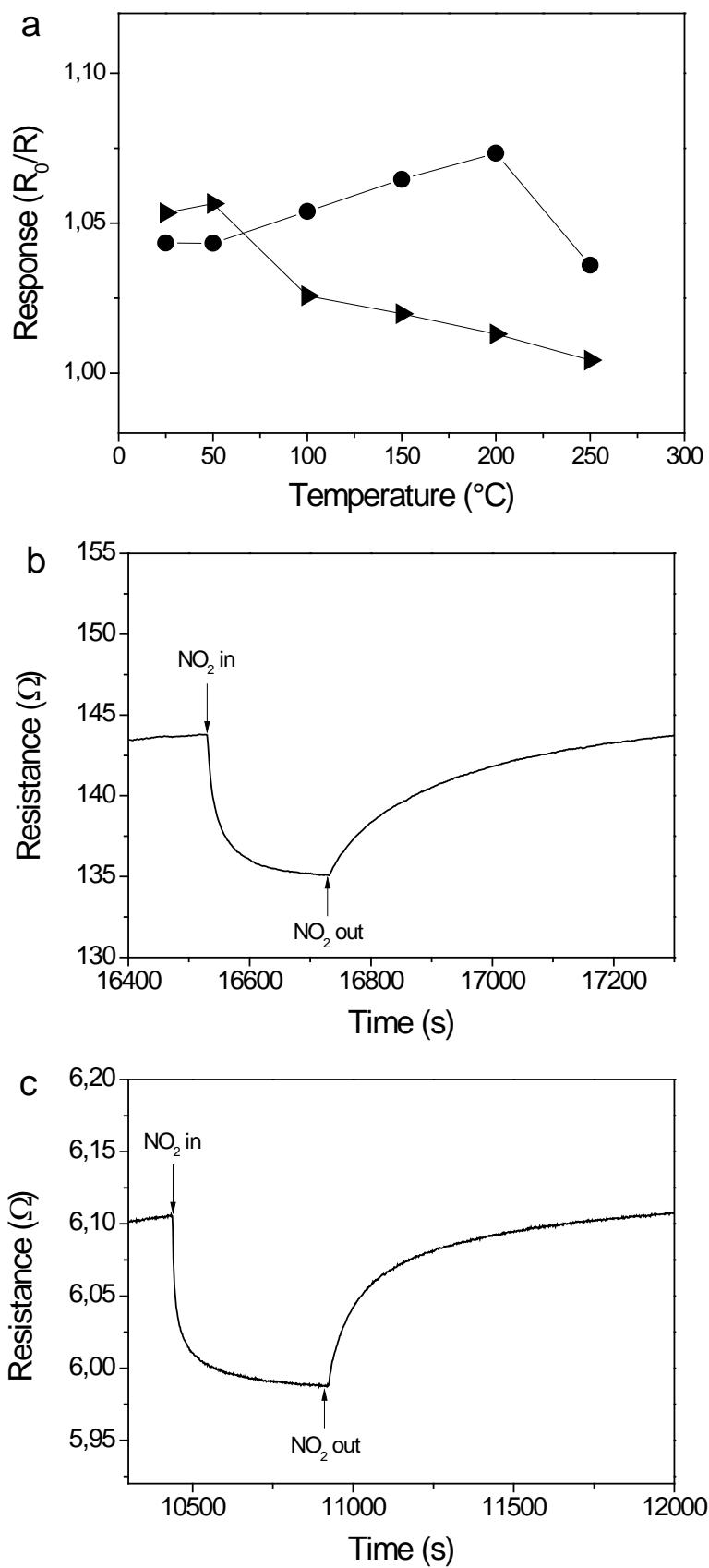


Figure S1. a) Sensor responses, toward 8 ppm of NO_2 , as a function of the operating temperature of uncoated CNT1500 (circles) and CNT3000 (triangles) sensors. Transient responses to 8 ppm of NO_2 at 150 $^{\circ}\text{C}$ of devices made of uncoated b) CNT700 and c) CNT3000 film.